REGULAR PAPER

DOI: 10.1007/s40684-018-0001-1
ISSN 2288-6206 (Print) / 2198-0810 (Online)

Evaluation of Energy Efficiency of Thermoelectric Generator with Two-Phase Thermo-Syphon Heat Pipes and Nano-Particle Fluids

Tahsin Atalay[1], Yavuz Köysal[2,#], Ali Ekber Özdemir[3], and Engin Özbaş[4]

1 Department of Electronics and Automation, Yeşilyurt Demir Çelik Vocational School, Ondokuz Mayıs University, Samsun, 55330, Turkey
2 Department of Electricity and Energy Technologies, Yeşilyurt Demir Çelik Vocational School, Ondokuz Mayıs University, Samsun, 55330, Turkey
3 Ship Machinery Bussiness Engineering Department, Fatsa Faculty of Marine Sciences, Ordu University, Ordu, 52400, Turkey
4 Department of Motor Vehicles and Transportation, Yeşilyurt Demir Çelik Vocational School, Ondokuz Mayıs University, Samsun, 55330, Turkey
Corresponding Author / E-mail: yavuzk@omu.edu.tr, TEL: +90-362-3121919

KEYWORDS: Thermoelectric generator, Heat pipe, Solar energy, Renewable energy, Solar collectors, Nano-particles

This paper investigates the effects of heat pipes filled with water and nanoparticles (MgO) on electricity generation. The experimental setup comprises of two-phase thermo-syphon heat pipes filled with water or MgO nanoparticle-water suspension, thermoelectric generator (TEG) modules and heat sinks that use passive and active cooling systems. Concentrated solar radiation with heat pipes was used as a heat source for heating. Specially constructed heat sinks with coolant tunnels were used for cooling. Heating and cooling processes are needed to create a temperature difference to generate electrical energy. The constructed model represents the influence of basic parameters such as the tilt angle of heat pipes, working fluids, cooling process, etc. on the maximum power generated. Systems in the constructed setup were arranged with a specific angle to the incident angle of solar radiation. The experiment was carried out on August 5th, 2015, in the northern coast of Turkey, city of Samsun with latitude of 41º14' N. The results obtained show that the presented experimental setup can be used to evaluate thermoelectric energy potential of local areas or to investigate optimum cooling or heating processes.

Manuscript received: October 18, 2016 / Revised: March 4, 2017 / Accepted: March 21, 2017

NOMENCLATURE

V_{oc} = Open circuit voltage (V)
T_h = Thermoelectric hot side temperature (ºC)
T_c = Thermoelectric cold side temperature (ºC)
ΔT = Temperature difference between hot and cold side of thermoelectric generator (ºC)
α_{TEG} = Effective Seebeck coefficient of the TE module
I_{st} = Received radiated power on solar collector tube (W)
η_e = Electrical efficiency (%)
P_{max} = Match load output power (W)
R_T = Thermal resistance of the heat pipe (ºC/W)

1. Introduction

It is a fact that developing technology causes an increase in energy usage, so energy generation is a very important factor in the world to ensure the continuance of technology. At the same time, the major problem of developing technology and hence humanity is meeting the ever increasing energy demand. Industrial buildings, factories, our homes, farms, all daily devices and vehicles need constant energy. Thus, it becomes necessary to investigate new energy sources to meet this energy demand. Nevertheless, more than 80% of the world's primary energy consumption is fossil fuels.[1] It is known that fossil fuel usage causes environmental problems. The most important of these environmental problems are global warming and air pollution. Renewable energy systems are the most important components of the strategy to reduce harmful emissions that endanger the future of Earth. Moreover, the fossil fuel sources are limited and won't be available forever. Renewable energy is defined as "energy generated by sources whose supplies are regenerative and virtually inexhaustible”[2,3] Electricity can be produced with different techniques.[4] However, some of these are not environmental-friendly. For instance, nuclear energy plants use nuclear reaction to produce electricity. Chernobyl(1986) and Fukushima(2011) accidents have had some unfavorable significant industrial, political, and national impacts worldwide. Because of major environmental problems and limited energy sources, renewable energy technologies have become more popular in the last decades.

There are many works about renewable energy production from wind, wave, bio-energy and geothermal etc. energies. In fact, all these energy sources are mainly based on the sun. However, electrical energy is produced indirectly from many of these energy sources. Since PV and TEG modules use solar power directly, they have become one of the most popular devices for generating clean energy.

A TEG module converts heat energy into electrical energy. It is possible to generate electrical energy using TEG modules which lets out waste heat.[5-8] Theoretical and experimental studies on producing electrical energy using solar power on TEG modules are also popular nowadays.[9-15] There are many studies related to the production of energy via TEG modules. Many of these studies are based on experimental works.[16-22]

The main objective of this study is to produce electrical energy via TEG modules using solar radiation. On the other hand, we also aim to investigate the effects of heat pipes filled with MgO nano-particles on selected tilt angles by the solar altitude. For this aim, we presented all the components and working principles of the new experimental setup constructed.

2. Experimental Components

2.1 Structure of Thermoelectric Module

The constructed experimental setup is based on thermoelectric energy produced by TEG modules. Therefore, the most important part of the presented experimental setup is the TEG modules. TEGs are special structures that convert temperature differences into DC electricity directly. A TEG module is comprised of a series of electrically connected semiconductor materials.

A TEG module produces electrical power under the Seebeck effect by heat flow across two sides of a TEG structure. The open circuit voltage produced is directly proportional to the temperature difference between the two sides of the TEG module. Seebeck coefficient (α_{TEG}) is expressed as;

$$\alpha_{TEG} = \frac{V_{oc}}{(T_h - T_c)} \quad (1)$$

where V_{oc} is the out circuit voltage, T_h is hot side temperature, T_c is cold side temperature of the TEG module.[23] Producing energy by TEG generators has some advantages over conventional methods. TEG modules have no moving parts, they are environmental-friendly and maintenance-free, etc. Therefore, there are many studies about the usage of TEG modules. Many of these studies are related to waste heat recovery.[24,25] However, TEG modules have wide application areas. For instance, NASA used TEG modules in the Voyager mission.[26] In addition, there are some studies which used TEG structures on human body applications.[27] In 1991, a watch company manufactured a product which provided energy from a micro TEG module.[28] Usage of TEG modules in the production of renewable energy is partly a new area. In this experimental setup, TEG1-12611-6.0 type modules having 56 mm length, 56 mm width and 4 mm height were used.

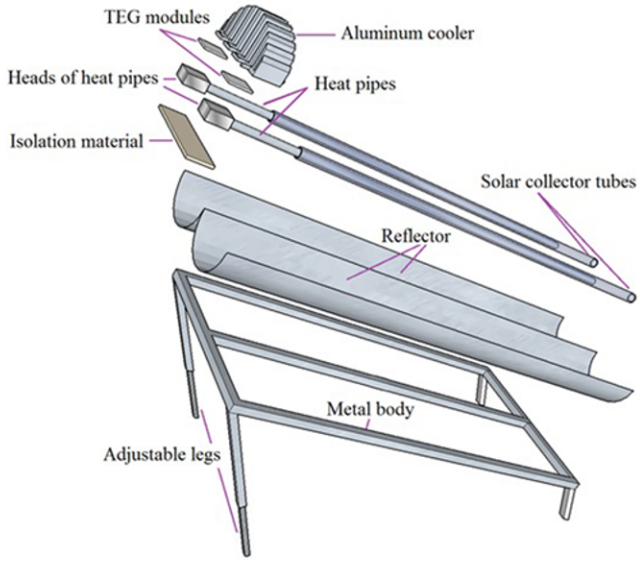

Fig. 1 The physical structure of the experimental setup

2.2 Preparation of Nanofluid

In this experimental setup, two types of working fluid were used for selected heat pipes. One of these working fluids was only water, while the other one was metal oxide nano particles in thin powder form MgO in water. Nanofluids contain metal oxides such as MgO_2, Al_2O_3, MgO etc., and they gain higher thermal conductivity in water when compared with the studied systems. Our purpose was to observe the effects of different working fluids on thermal conductivity of heat pipes, and hence electricity generation in the system. Many experimental studies performed nanofluids and nanoparticles in various systems including heat pipes.[29,30]

The prepared working nanofluid had 2% metal-oxide MgO nanoparticle content (7,2 g). The ultrasonic process was applied with SONICS VCX 750 ultrasonic processor with the probe diameter of 25 mm. When ultrasonic process was applied only for five minutes it was observed that sedimentation was uncontrollable. To avoid sedimentation of the nanoparticles, ultrasonication process was applied for 40 minutes. At the end of the first ten minutes the obtained energy was 45780 J, conductivity was 330 μs/cm and temperature was 33,7°C. At the end of the ultrasonic process of 40 minutes, the energy obtained was 41870 J, conductivity was 257,5 μs/cm and temperature was 53,7°C. Nanofluid with suspended particles was obtained after the final process.

2.3 Constructed System

It is known that thermoelectric generators need an absolute temperature difference between the two sides of the module to produce energy. In this study, the required temperature difference was obtained from solar radiation and specific cooling processes. Solar radiation was

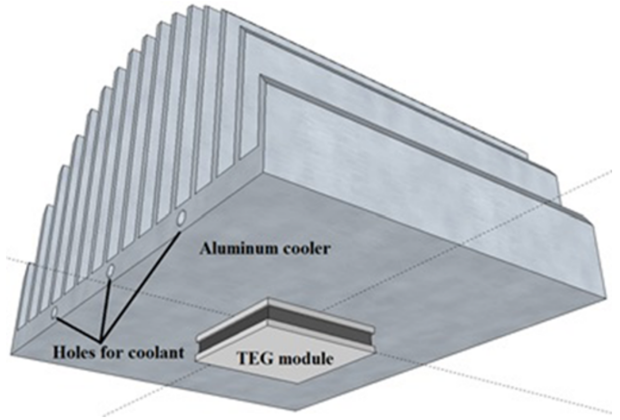

Fig. 2 The physical details of the aluminum cooler

concentrated via solar collector tubes and reflectors for the heating process. Concentrated solar radiation was converted into heat by heat pipes. The obtained heat was transferred to the TEG module by the head of the heat pipe. Cooling was achieved by specially designed aluminum heat sinks. The physical structure of constructed experimental setup is given in Fig. 1.

The aluminum heat sink prepared for the cooling process is shown in Fig. 2. This heat sink had three tunnels extending from one side to the other of aluminum block. These tunnels were used for an affective cooling. In the heat sinks, the distances between these tunnels and the diameters of tunnel holes were arranged equally. Efficient cooling was obtained with these tunnels using coolant of water. At the same time, passive cooling process was enhanced with the fins of the aluminum cooler using wind. A TEG module was placed on the bottom-center of the aluminum cooler as seen in Fig. 2. Other sides of the used TEG modules were tightly connected to the head of the heat pipes and thermal conductivity was quarantined with thermal greases on both sides of the TEG modules.

Heating and cooling parts of the experimental setup mounted are seen in Fig. 3. Another important part of the constructed experimental setup is solar collector tubes. Solar radiation was concentrated with these tubes. Solar collector tubes used in the system consist of evacuated glass tubes which have 1.8 m length, 37 mm inner diameter with 0.209 m^2 surface area. These solar collector tubes are standard commercial products and are easily accessible. Also it is possible to produce specifically designed solar tubes to evaluate and observe the solar collectors' effect.

A standard thermo-syphon type heat pipe consists of a vacuumed metal tube which includes a little working fluid. This type of heat pipes doesn't need any wick because they work under gravity. Concentrated solar radiation rises up the temperature of the heat pipe used and evaporates the little amount of working fluid. The resulting vapor moves rapidly towards the head of the heat pipe as a heat source. The high temperature obtained from the heat pipe is transferred to the hot side of the TEG module. The heat pipe and head of the heat pipe are shown in Fig. 4.

Thermal isolation precautions were taken to prevent heat loss in the system. Each heat pipe was equipped with thermocouples for data acquisition. Heat pipes were combined with thermal isolation materials

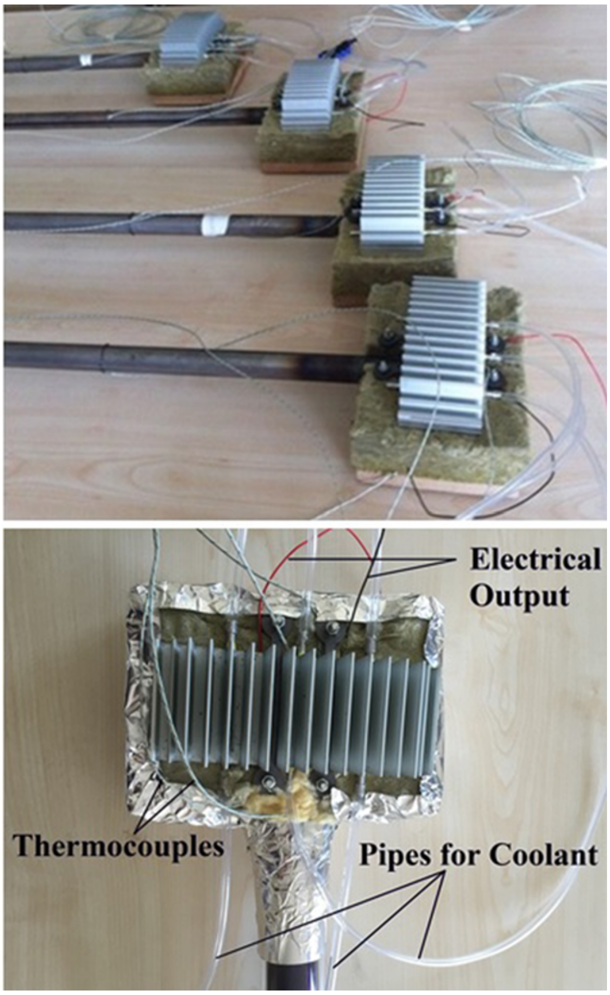

Fig. 3 Heating parts and aluminum cooler with all components

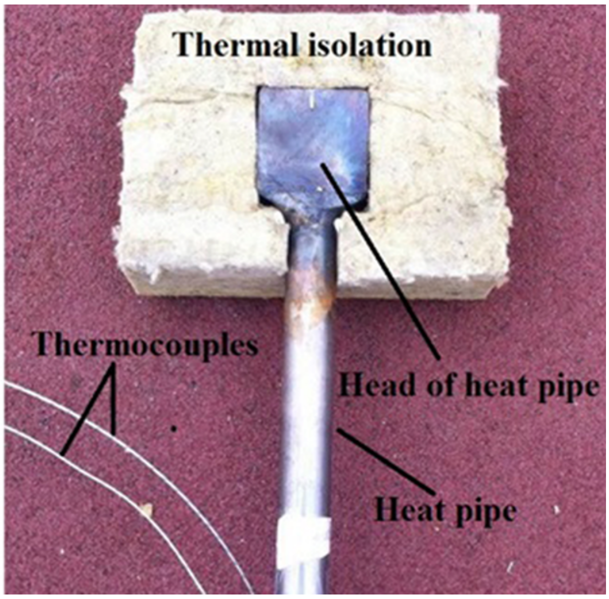

Fig. 4 Heat pipe with thermal isolation material

for an efficient thermal transfer.

A multiple system was set to obtain the effects of different working

Fig. 5 The constructed experimental setup

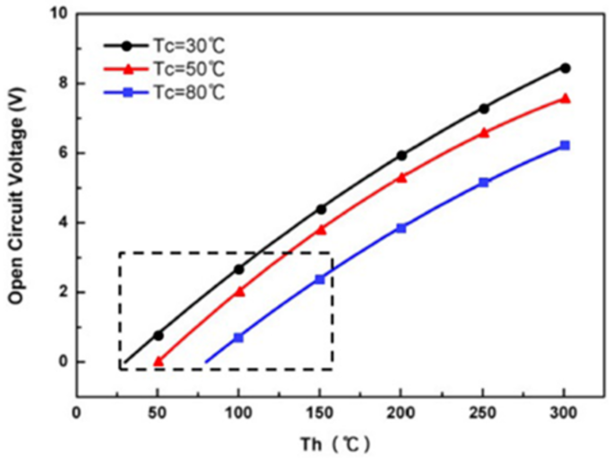

Fig. 6 Thermoelectric open circuit voltage condition versus temperature

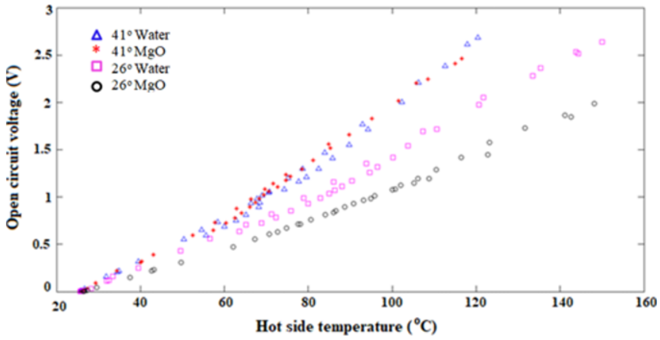

Fig. 7 Open circuit voltage characteristics of the heat pipes with working fluid used

fluids and slope of heat pipes against generated voltage. It is known that to obtain a good summer performance, the collector of a system should be mounted at the angle of ϕ-15 for summer time and ϕ+15 for winter time[31] where ϕ is latitude or angular distance from the equator of the experiment location. Depending on the location where the experimental system was constructed the tilt angles were arranged to 26 and 41 degrees to see the summer performance of the latitude angle.

In the system, two heat pipes were filled with water and the two other heat pipes were filled with MgO nanoparticle/water. Two heat pipes filled with water and MgO nanoparticle/water were set up to 26 degree tilt angle and the other two groups were set up to 41 degree tilt angle. In this manner, it is possible to measure different quantities such as open circuit voltage, hot and cold side temperature, simultaneously. In this system, each heat pipe was equipped with five K-type thermocouples which were connected to a data logger (ORDEL UDL 100 with the accuracy of 0.2%). Three of these thermocouples were placed in equal distances along the heat pipes. The other two of these thermocouples were placed on the hot and cold sides of the TEG modules.

Additionally, two thermocouples were located at two sides of the tunnels to measure the entrance and exit temperatures of the coolant water. Furthermore, a thermocouple was used to measure the ambient temperature. To measure solar radiation values, a pyranometer (DeltaOhm LP PYRA02) was used. All collected measurements were recorded to a computer in real time via data loggers. Mirror reflectors were used in this system to concentrate secondary reflections on to the heat pipes. The multiple system setup constructed is shown in Fig. 5.

3. Experimental Results

3.1 Open Circuit Voltage Generated

In this part, we aimed to reveal the relationship between the open circuit voltage and the hot and cold side temperature differences of the TEG module. For this purpose, related electrical parameters were collected such as open circuit voltage and temperature difference. The parameters collected were compared with the characteristic values of the TEG modules used mentioned in Fig. 6, which were provided by the producing company.

Fig. 6 is concerned with open circuit voltage-hot side characteristic of the TEG module. As shown in this Fig. 6, to create significant voltage value, it is important to fix the temperature of the cold side of this module as low as possible. It is known that electrical energy generated via TEG module is related with the temperature difference of the sides of module. However, it should be noted that it is critical for the temperature of the cold side to be as low as possible. For a given temperature difference in a module, electrical efficiency is more active for TEG module when the cold side temperature is as low as possible. In this graphic, it is seen that black, red and blue lines give some information about the open circuit voltage value, thereby the generated power. The black line is of course the most intended temperature line for electrical generation. In the experimental setup, the cold side of the TEG module was cooled by an aluminum cooler which contains coolant tunnels. In this case, the cold side temperature of the TEG module was fixed as low as possible in an experiment day. The generated voltage values corresponding to these temperature values were obtained around 2-2.7 volts in noon time. When the obtained values are compared with the given graphic of the TEG module, it is seen that experimental values measured are consistent with the related graphic. In Fig. 7, the open circuit voltage values are increasing with the hot side temperature of the TEG module almost linearly.

This is another proof of consistency of measurements. It is also seen that systems of heat pipes at the angle of 41 degree were more effective

Table 1 Some calculated electrical parameters at an angle of 41 degrees

Heat pipe at a tilt angle of 41 degrees with working fluid water					
Time	I_{st}	α_{TEG}	P_{max}	η_e	R_T
10:00-10:15	61,11	0,031	0,010	0,016	0,664
10:30-10:45	129,70	0,028	0,065	0,050	0,277
11:00-11:15	147,18	0,028	0,113	0,077	0,261
11:30-11:45	183,78	0,030	0,235	0,128	0,170
12:00-12:15	186,97	0,031	0,354	0,189	0,165
12:30-12:45	187,79	0,034	0,653	0,348	0,182
13:00-13:15	189,90	0,037	1,425	0,750	0,233
13:30-13:45	159,54	0,036	1,187	0,744	0,230
14:00-14:15	173,35	0,032	0,614	0,354	0,182
14:30-14:45	163,03	0,030	0,417	0,256	0,188
15:00-15:15	150,15	0,029	0,306	0,204	0,207
15:30-15:45	118,09	0,028	0,244	0,207	0,274
16:00-16:15	112,86	0,030	0,216	0,191	0,320

Heat pipe at a tilt angle of 41 degrees with working fluid containing MgO nanoparticles					
Time	I_{st}	α_{TEG}	P_{max}	η_e	R_T
10:00-10:15	61,11	0,025	0,020	0,033	0,519
10:30-10:45	129,70	0,025	0,075	0,057	0,262
11:00-11:15	147,18	0,027	0,160	0,108	0,231
11:30-11:45	183,78	0,028	0,246	0,134	0,193
12:00-12:15	186,97	0,029	0,317	0,170	0,205
12:30-12:45	187,79	0,032	1,015	0,540	0,293
13:00-13:15	189,90	0,032	1,210	0,637	0,284
13:30-13:45	159,54	0,031	0,846	0,530	0,295
14:00-14:15	173,35	0,030	0,575	0,332	0,238
14:30-14:45	163,03	0,028	0,403	0,247	0,228
15:00-15:15	150,15	0,028	0,310	0,206	0,232
15:30-15:45	118,09	0,027	0,254	0,215	0,277
16:00-16:15	112,86	0,026	0,218	0,193	0,286

Table 2 Some calculated electrical parameters at an angle of 26 degrees

Heat pipe at a tilt angle of 26 degrees with working fluid water					
Time	I_{st}	α_{TEG}	P_{max}	η_e	R_T
10:00-10:15	61,11	0,026	0,005	0,009	0,831
10:30-10:45	129,70	0,023	0,039	0,030	0,390
11:00-11:15	147,18	0,022	0,104	0,071	0,269
11:30-11:45	183,78	0,023	0,203	0,111	0,158
12:00-12:15	186,97	0,025	0,381	0,204	0,145
12:30-12:45	187,79	0,026	0,875	0,466	0,124
13:00-13:15	189,90	0,026	1,336	0,704	0,139
13:30-13:45	159,54	0,026	1,319	0,827	0,174
14:00-14:15	173,35	0,025	0,815	0,470	0,196
14:30-14:45	163,03	0,024	0,495	0,304	0,196
15:00-15:15	150,15	0,023	0,363	0,241	0,190
15:30-15:45	118,09	0,022	0,286	0,242	0,236
16:00-16:15	112,86	0,021	0,239	0,212	0,247

Heat pipe at an tilt angle of 26 degrees with working fluid containing MgO nanoparticles					
Time	I_{st}	α_{TEG}	P_{max}	η_e	R_T
10:00-10:15	61,11	0,016	0,011	0,019	0,535
10:30-10:45	129,70	0,016	0,047	0,036	0,224
11:00-11:15	147,18	0,016	0,083	0,057	0,213
11:30-11:45	183,78	0,016	0,146	0,080	0,176
12:00-12:15	186,97	0,017	0,244	0,131	0,192
12:30-12:45	187,79	0,017	0,299	0,159	0,213
13:00-13:15	189,90	0,019	0,710	0,374	0,307
13:30-13:45	159,54	0,019	0,726	0,455	0,339
14:00-14:15	173,35	0,019	0,518	0,299	0,251
14:30-14:45	163,03	0,018	0,345	0,212	0,233
15:00-15:15	150,15	0,017	0,265	0,176	0,235
15:30-15:45	118,09	0,017	0,214	0,181	0,286
16:00-16:15	112,86	0,017	0,180	0,159	0,288

than those at 26 degrees in the morning time depending on the solar altitude angle. Two different heat pipes filled with only water or filled with MgO nanoparticles in water also showed different characteristics according to the solar altitude angle. The heat pipe filled with MgO nanoparticles in water was more effective than other heat pipes in terms of generating voltage from morning till noon time. When the systems were at a steady state just before the noon of the experiment day, the voltage generations were almost the same for both heat pipes at 41 degrees. However, same results were not obtained for the heat pipes with tilt angles of 26 degrees. As seen from Fig. 8, the same efficiency could not be obtained with the heat pipes filled with water or MgO nanopartical in water at 26 degrees. All these values obtained are related to the angle of incidence of solar radiation during the experiment day. It is well known that the voltage generated is directly proportional with the temperature difference with the hot side and cold side of the TEG module. Also, it is important to fix the cold side temperature as low as possible as shown in Fig. 6. To create an efficient cooling, the cold side of the TEG module was combined with the aluminum heat sink. Cooling water was allowed to flow through the cylindrical tunnels of the heat sink. In this manner, it was almost possible to fix the cold side temperature against hot side of the TEG module. The accessible voltage values corresponding to the hot side values of TEG module are indicated with black-dashed line area in Fig. 6. This means that the voltage generated is related with the temperature difference (ΔT) between the sides of the TEG module.

Maximum power (P_{max}) and electrical efficiency (η_e) can be calculated with collected data which are selected from average values of fifteen minutes interval. These electrical parameters were calculated using the equations below:[17,32]

Maximum power output that obtained at matched load is;

$$P_{max} = \frac{V_{oc}^2}{4R} \tag{2}$$

where V_{oc} is the open circuit voltage, and R is the internal resistance value (1.2 Ω) of the experimental TEG module used. Electrical efficiency (η_e) of the TEG module can be calculated using the calculated values of maximum output power (P_{max}) and solar irradiation (I_{st}) collected by the solar collector tube in the experimental system;

$$\eta_e = \frac{P_{max}}{I_{st}} \times 100 \tag{3}$$

Tables 1 and 2 summarize some electrical parameters calculated as mentioned above.

These calculated values belong to average of fifteen minutes intervals. To eliminate rapidly changing values we used fifteen minutes intervals on average.

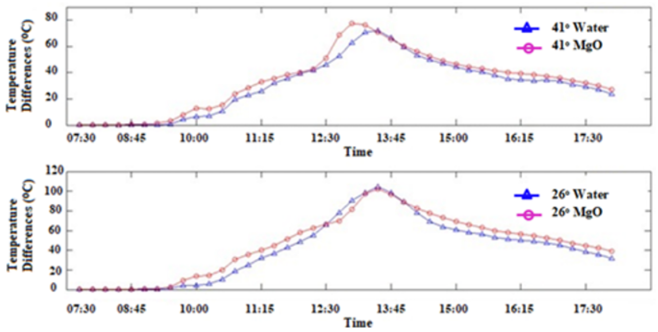

Fig. 8 The temperature differences obtained from TEG modules according to the heat pipes

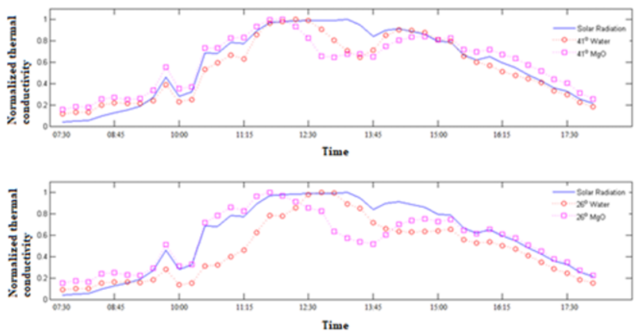

Fig. 9 Normalized values of thermal conductivity with solar radiation

It is seen from the Tables 1 and 2 that, generally, maximum efficiency is related to the intensity of solar radiation as expected. Despite that, some of the efficiency values are seen to be incompatible with related solar radiation values. This situation is expected and it is due to the change in the weathers, instantaneously. Here, the average values were selected for this reason. Starting from the morning, the temperature difference on the two sides of the TEG module increased gradually in each related time period. The TEG modules at the tilt angle of 41 degrees act more efficiently in terms of generating electricity when compared with other modules at the tilt angle of 26 degrees. Just before the noon time, it was observed that the generating characteristics of heat pipes changed in relation to the solar altitude angle. In the early afternoon, related to the solar altitude angle, the TEG modules at the tilt angle of 26 degrees obtained more temperature difference than the modules at the tilt angle of 41 degrees. The temperature difference of the TEG modules used reached maximum values in the early afternoon, between 12:30 and 13:45. In this time period, calculated electrical parameters reached maximum power with matched load ($P_{\max}$), Seebeck coefficient (α_{TEG}) and electrical efficiency (η_e) reached maximum values and as a result, the open circuit voltage values were measured with the maximum values. Heat pipes with nano-particles were a slightly more efficient in terms of electrical efficiency until noon time. However, it was seen that afternoon time heat pipes with only water were more efficient. The details of temperature differences obtained from the TEG modules are shown in Fig. 8.

A remarkable declination started around 9 a.m. in the morning and such a trend was fairly observed around 12:30 in early afternoon for all the systems at a tilt angle of 26 and 41 degrees. It was also observed that temperature differences were rapidly rising up for both angles of 41 degrees and 26 degrees in heat pipe systems. Nevertheless, it was also observed that the systems with the tilt angle of 26 reached higher temperature differences. Starting from the afternoon, temperature differences gradually decreased for all the systems.

3.2 Thermal Conductivity of the Heat Pipes with Working Fluids under Different Tilt Angles

The thermal resistance of the system used is an important parameter which affects the performance of the heat pipe. The thermal resistance (R_T) between the evaporator and condenser sections is defined as:[33]

$$R_T = \frac{\Delta T}{\dot{Q}_e} \tag{4}$$

where $\dot{Q}_e$ is the received solar heating power by the solar collector tube which is called (I_{st}). (ΔT) was obtained from temperature difference between the mean temperature of the evaporator and condenser sections. In order to map out the thermal characteristic of the heat pipes with different working fluids, a certain number of thermocouples were used for specified points on the heat pipes. To calculate average temperature, two local points (close to the upper and lower regions of the heat pipe) were selected on the evaporator section, and hot side of the head of the heat pipe was selected as the local point for the condenser section. Thus, ΔT is given by:

$$\Delta T = \left(\frac{T_{eva(upper)} + T_{eva(lower)}}{2}\right) - (T_{con(hot\ side)}) \tag{5}$$

It is known that the reciprocal of thermal resistance is thermal conductivity. Steady-state temperature profiles of the systems used are shown in Fig. 9. To show thermal conductivity and solar radiation values in the same scale, they were given by normalized values (between 0 and 1).

It is seen from the graphics that the thermal conductivity of all systems were increasing or decreasing with increases or decreases in solar radiation, regardless of working fluid or tilt angles. Thermal conductivity reaches maximum values with the maximum temperature difference at noon time. Despite this, it reaches minimum values in the evening, like early in the morning.

To obtain a good summer performance, the heat pipes of the constructed system were mounted at the angle of ϕ-15, where ϕ is the latitude or angular distance from the equator of the experiment location. As a result of this, the tilt angles of the constructed systems were set up to 26 and 41 degrees in relation to the geographical location of the city of Samsun with latitude of 41°14′ N. In this experimental system, calculated $P_{\max}$ is dependent on the obtained V_{oc} values. Furthermore, it is also known that V_{oc} is dependent on the temperature difference between the hot side and cold side of the TEG module. The hot side of the TEG module is related to solar irradiation and the cold side is related to the effective cooling system. So, it could be said that V_{oc} depends on all other systematic parameters indirectly. When the heat pipes that belong to the system at the tilt angle of 41 degrees were compared with each other, it was observed that the heat pipe with nanoparticles reached the higher $P_{\max}$ earlier than the heat pipe filled with only water. This can be interpreted as MgO nanoparticle being a better thermal conductor than water. The same results were not observed in other system at the tilt angle of 26 degrees. This was an expected situation related to the solar altitude angle. In the morning hours, incoming solar irradiation beams are not normal to the collector tube with the systems at the angle of 26 degrees. So, the expected P_{max} values did not occur until noon hours for both heat pipes filled with water or MgO nanoparticles.

4. Conclusions

The purpose of this paper was to analyze TEG modules mounted on water filled and MgO Nano-fluid filled two-phase thermo-syphon heat pipes. It is known that heat pipes with evacuated tubes are good agents for thermal energy harvested from the Sun. This thermal energy obtained can be used for thermoelectric energy production. It is possible to come across a great number of studies related with heat pipes in the literature; however, there are few studies on heat pipes integrated with TEG modules. This study is different from others in terms of the established location, working fluid used and constructed tilt angle. This way, it is possible to reveal the efficiency of the TEG modules used for generating electrical power dependent on other parameters such as working fluid, tilt angles, coolant system etc. In this study, it was planned to analyze the generated open circuit voltages with different working fluids and under different tilt angles. The collected experimental parameters such as solar irradiation, open circuit voltage, hot and cold side temperature were interpreted with selected working fluids and tilt angles. Some electrical and thermal quantities such as maximum power with matched load (P_{max}), Seebeck coefficient (α_{TEG}), electrical efficiency (η_e) and thermal resistance (R) were calculated by using collected experimental data. The obtained results show that, it is possible to generate electrical energy by using constructed system. However, constructed system is to be evaluated for using multi TEG modules for generating usable electrical energy. Also, this system gives some information about the necessity of the nano-particles for working fluid used. Our experiments show that water is sufficient for use as working fluid according to climactic geography of the constructed system. It means that there is no need to use nano-particles for working fluid used where the location is near to aclinic line. However, it may be useful for locations away from the aclinic line. Obtained results and calculated quantities were given with graphics and tables. Furthermore, it was also observed that the obtained results were consistent with each other. This experimental system gives information about how to generate electrical energy and how to change the total amount of generated energy by changing the dependent parameters.

Conflict of Interests

On behalf of all authors, the corresponding author states that there is no conflict of interest.

REFERENCES

1. Rosenfel, A., McAuliffe, P., and Wilson, J., "Energy Efficiency and Climate Change," Reference Module in Earth Systems and Environmental Sciences, pp. 373-382, 2004.
2. Arizona Solar Center, "Renewable Energy: An Overview," https://azsolarcenter.org/renewable-energy-an-overview (Accessed 21 DEC 2017).
3. Park, E. and Ohm, J. Y., "Factors Influencing the Public Intention to Use Renewable Energy Technologies in South Korea: Effects of the Fukushima Nuclear Accident," Energy Policy, Vol. 65, pp. 198-211, 2014.
4. Bhandari, B., Poudel, S. R., Lee, K.-T., and Ahn, S.-H., "Mathematical Modeling of Hybrid Renewable Energy System: A Review on Small Hydro-Solar-Wind Power Generation," Int. J. Precis. Eng. Manuf.-Green Tech., Vol. 1, No. 2, pp. 157-173, 2014.
5. Heghmanns, A., Beitelschmidt, M., Wilbrecht, S., Geradts, K., and Span, G., "Development and Optimization of a TEG-System for the Waste Heat Usage in Railway Vehicles," Materials Today: Proceedings, Vol. 2, No. 2, pp. 780-789, 2015.
6. Mal, R., Prasad, R., Vijay, V. K., and Verma, A. R., "The Design, Development and Performance Evaluation of Thermoelectric Generator (TEG) Integrated Forced Draft Biomass Cookstove," Procedia Computer Science, Vol. 52, pp. 723-729, 2015.
7. Orr, B., Akbarzadeh, A., Mochizuki, M., and Singh, R., "A Review of Car Waste Heat Recovery Systems Utilising Thermoelectric Generators and Heat Pipes," Applied Thermal Engineering, Vol. 101, pp. 490-495, 2016.
8. Chávez-Urbiola, E., Vorobiev, Y. V., and Bulat, L., "Solar Hybrid Systems with Thermoelectric Generators," Solar Energy, Vol. 86, No. 1, pp. 369-378, 2012.
9. Zhang, Z., Li, W., and Kan, J., "Behavior of a Thermoelectric Power Generation Device Based on Solar Irradiation and the Earth's Surface-Air Temperature Difference," Energy Conversion and Management, Vol. 97, pp. 178-187, 2015.
10. Shen, Z.-G., Wu, S.-Y., Xiao, L., and Yin, G., "Theoretical Modeling of Thermoelectric Generator with Particular Emphasis on the Effect of Side Surface Heat Transfer," Energy, Vol. 95, pp. 367-379, 2016.
11. Li, G., Zhang, G., He, W., Ji, J., Lv, S., et al., "Performance Analysis on a Solar Concentrating Thermoelectric Generator Using the Micro-Channel Heat Pipe Array," Energy Conversion and Management, Vol. 112, pp. 191-198, 2016.
12. Chen, W.-H., Wang, C.-C., Hung, C.-I., Yang, C.-C., and Juang, R.-C., "Modeling and Simulation for the Design of Thermal-Concentrated Solar Thermoelectric Generator," Energy, Vol. 64, pp. 287-297, 2014.
13. Kossyvakis, D., Vossou, C., Provatidis, C., and Hristoforou, E., "Computational Analysis and Performance Optimization of a Solar Thermoelectric Generator," Renewable Energy, Vol. 81, pp. 150-161, 2015.
14. Jaworski, M., Bednarczyk, M., and Czachor, M., "Experimental Investigation of Thermoelectric Generator (TEG) with PCM Module," Applied Thermal Engineering, Vol. 96, pp. 527-533, 2016.

15. He, W., Su, Y., Wang, Y., Riffat, S., and Ji, J., "A Study on Incorporation of Thermoelectric Modules with Evacuated-Tube Heat-Pipe Solar Collectors," Renewable Energy, Vol. 37, No. 1, pp. 142-149, 2012.

16. Date, A., Date, A., Dixon, C., and Akbarzadeh, A., "Theoretical and Experimental Study on Heat Pipe Cooled Thermoelectric Generators with Water Heating Using Concentrated Solar Thermal Energy," Solar Energy, Vol. 105, pp. 656-668, 2014.

17. Özdemir, A. E., Köysal, Y., Özbaş, E., and Atalay, T., "The Experimental Design of Solar Heating Thermoelectric Generator with Wind Cooling Chimney," Energy Conversion and Management, Vol. 98, pp. 127-133, 2015.

18. Yadav, S., Yamasani, P., and Kumar, S., "Experimental Studies on a Micro Power Generator Using Thermo-Electric Modules Mounted on a Micro-Combustor," Energy Conversion and Management, Vol. 99, pp. 1-7, 2015.

19. Singh, G., "A Six-Phase Synchronous Generator for Stand-Alone Renewable Energy Generation: Experimental Analysis," Energy, Vol. 36, No. 3, pp. 1768-1775, 2011.

20. Göllei, A., Görbe, P., and Magyar, A., "Measurement Based Modeling and Simulation of Hydrogen Generation Cell in Complex Domestic Renewable Energy Systems," Journal of Cleaner Production, Vol. 111, pp. 17-24, 2016.

21. Hussain, M. I. and Lee, G. H., "Experimental and Numerical Studies of a U-Shaped Solar Energy Collector to Track the Maximum CPV/T System Output by Varying the Flow Rate," Renewable Energy, Vol. 76, pp. 735-742, 2015.

22. Afshin, M., Sohankar, A., Manshadi, M. D., and Esfeh, M. K., "An Experimental Study on the Evaluation of Natural Ventilation Performance of a Two-Sided Wind-Catcher for Various Wind Angles," Renewable Energy, Vol. 85, pp. 1068-1078, 2016.

23. Rowe, D. M., "CRC Handbook of Thermoelectrics," CRC Press, 1995.

24. Hsiao, Y., Chang, W., and Chen, S., "A Mathematic Model of Thermoelectric Module with Applications on Waste Heat Recovery from Automobile Engine," Energy, Vol. 35, No. 3, pp. 1447-1454, 2010.

25. Niu, X., Yu, J., and Wang, S., "Experimental Study on Low-Temperature Waste Heat Thermoelectric Generator," Journal of Power Sources, Vol. 188, No. 2, pp. 621-626, 2009.

26. Snyder, G. J., "Small Thermoelectric Generators," The Electrochemical Society Interface, Vol. 17, No. 3, p. 54, 2008.

27. Jo, S., Kim, M., Kim, M., and Kim, Y., "Flexible Thermoelectric Generator for Human Body Heat Energy Harvesting," Electronics Letters, Vol. 48, No. 16, pp. 1015-1017, 2012.

28. Kishi, M., Nemoto, H., Hamao, T., Yamamoto, M., Sudou, S., et al., "Micro Thermoelectric Modules and their Application to Wristwatches as an Energy Source," Proc. of Eighteenth International Conference, pp. 301-307, 1999.

29. Sözen, A., Variyenli, H. İ., Özdemir, M. B., Gürü, M., and Aytaç, İ., "Heat Transfer Enhancement Using Alumina and Fly Ash Nanofluids in Parallel and Cross-Flow Concentric Tube Heat Exchangers," Journal of the Energy Institute, Vol. 89, No. 3, pp. 414-424, 2016.

30. Solomon, A. B., Ramachandran, K., and Pillai, B., "Thermal Performance of a Heat Pipe with Nanoparticles Coated Wick," Applied Thermal Engineering, Vol. 36, pp. 106-112, 2012.

31. Messenger, R. and Abtahi, A., "Photovoltaic Systems Engineering," CRC Press, 2017.

32. Nia, M. H., Nejad, A. A., Goudarzi, A., Valizadeh, M., and Samadian, P., "Cogeneration Solar System Using Thermoelectric Module and Fresnel Lens," Energy Conversion and Management, Vol. 84, pp. 305-310, 2014.

33. Peyghambarzadeh, S., Shahpouri, S., Aslanzadeh, N., and Rahimnejad, M., "Thermal Performance of Different Working Fluids in a Dual Diameter Circular Heat Pipe," Ain Shams Engineering Journal, Vol. 4, No. 4, pp. 855-861, 2013.